Supporting Information

Dray et al. 10.1073/pnas.0900222106

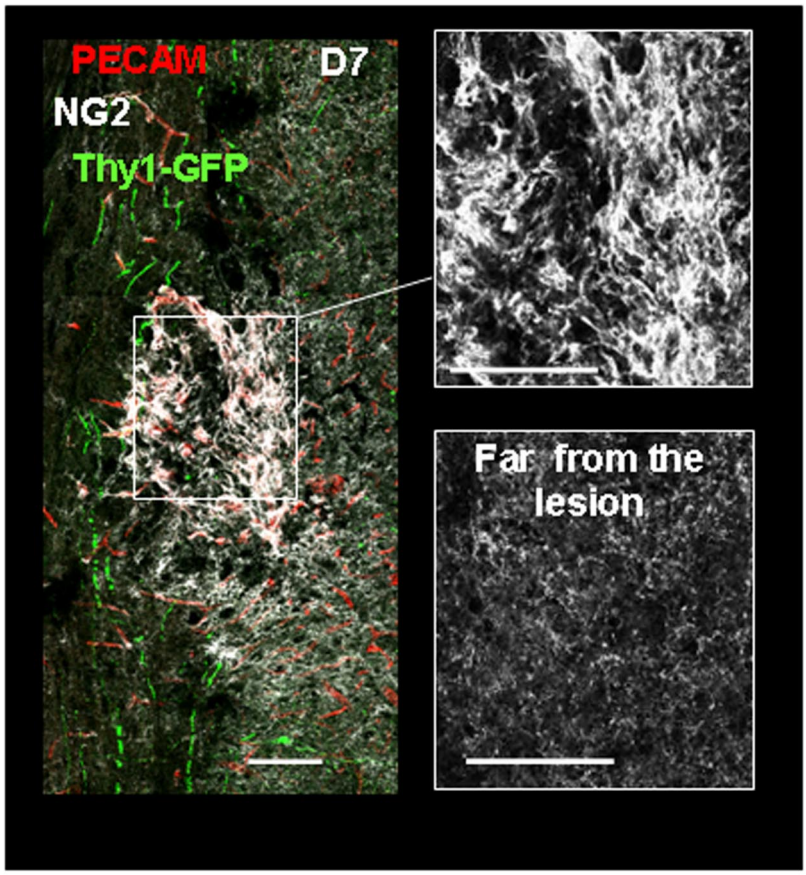

Pecam-NG2 Immunostaining at lesion site

Fig. S1. PECAM-NG2 immunostaining at the lesion site. Horizontal spinal cord section immunostained against PECAM (vessels, red) and NG2 chondroitin sulfate proteoglycan (NG2, white; GFP axons, green) on D7 after lesion.

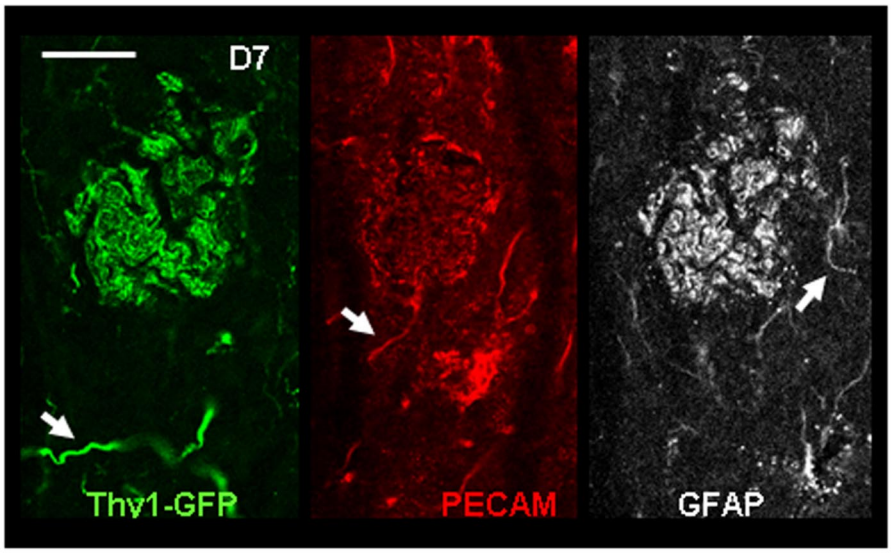

Localized autofluorescence at the lesion site

Fig. S2. Localized autofluorescence at the lesion site. Confocal image of the same fixed spinal cord slice as in Fig. 1*E* showing localized wide spectrum autofluorescence at the lesion site mostly in the GFAP and Thy1GFP channels. Note that true GFP, PECAM, and GFAP signals (arrows) were only visible in the dedicated channel. (Scale bar, 25 μm.)

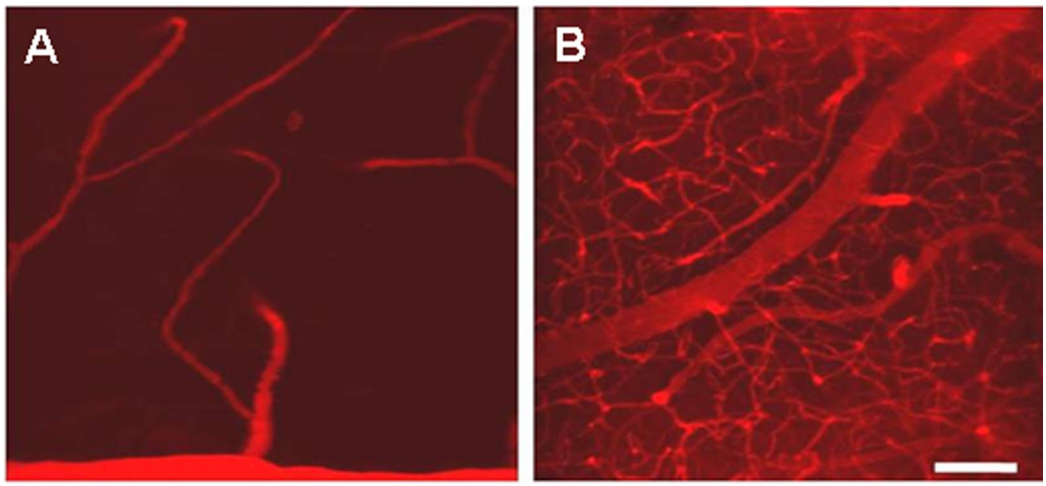

Spinal and cortical vascular networks

Fig. S3. Spinal and cortical vascular networks. Comparison of vascular networks in the dorsal columns of mouse spinal cord (*A*) and in mouse somatosensory cortex (*B*). Average projection of images acquired every 5 μm over 200 μm from the surface. (Scale bar, 100 μm.) Using X-ray CT-scanner together with sophisticated algorithms [Risser L, et al. (2007) From homogeneous to fractal normal and tumorous microvascular networks in the brain. *J Cereb Blood Flow Metab* 27:293–303] estimated that blood vessel volume represented about 2% of the overall cortex volume. Blood vessel volume in the dorsal spinal cord would therefore represent much less than 2% of the total volume. Given a 5-fold increase of blood vessel density after lesion, vascular scaffold would still occupy less than 10% of the total spinal cord volume. In case of random elongation 90% of the regenerative axon sprouts should thus be growing in the brain parenchyma. In fact, less than 50% were elongating more than 5 μm away from vessel surfaces supporting a marked preference of axon sprouts for the blood vessel environment versus brain parenchyma.

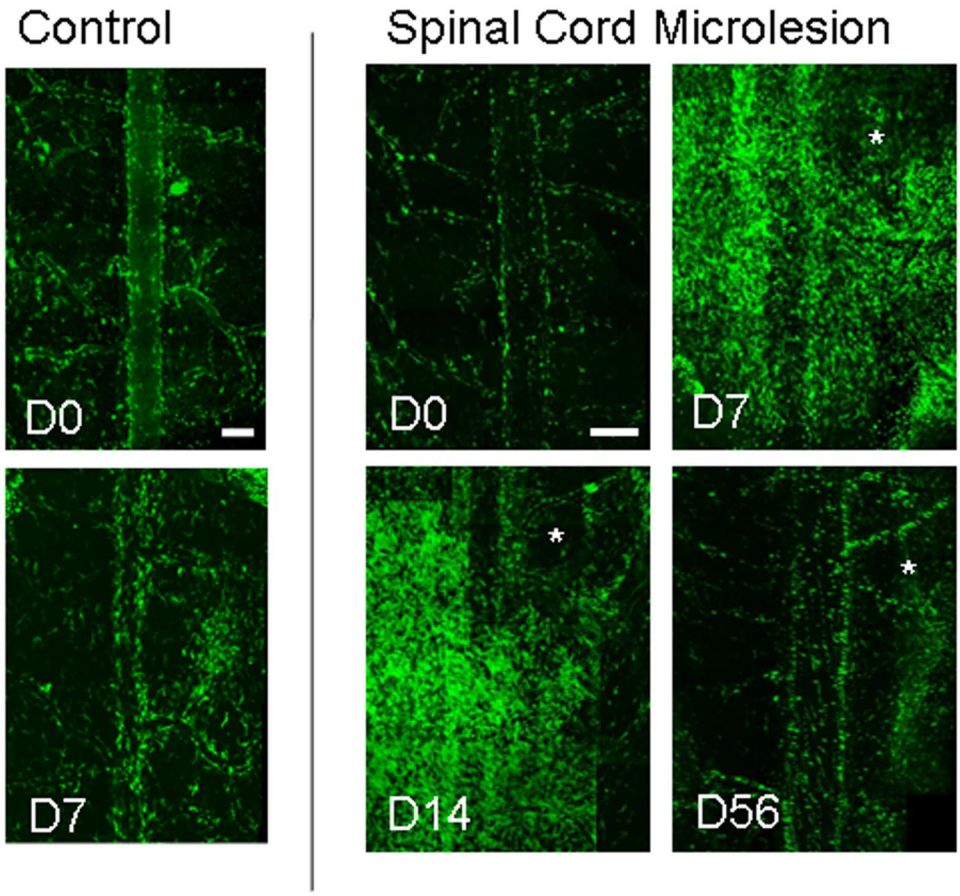

Macrophages recruitement in control conditions and after spinal cord microlesion.

Fig. S4. Macrophage recruitment in control conditions and after spinal cord microlesion. heGFP mice with GFP-labeled macrophages [Faust N, et al. (2000) Insertion of enhanced green fluorescent protein into the lysozyme gene creates mice with green fluorescent granulocytes and macrophages. *Blood* 96:719–26] were repeatedly imaged in control conditions and following dorsal column microlesion. Microlesion triggered massive and widespread macrophage recruitment over the first 2 weeks ($n = 2/2$), which was not observed in control mice ($n = 2/2$). (Scale bar, 100 μm.) Absence of focal recruitment, and slow recovery, suggest that macrophages would not be the only cause of the secondary degeneration of axons observed in Thy1-GFP mice.

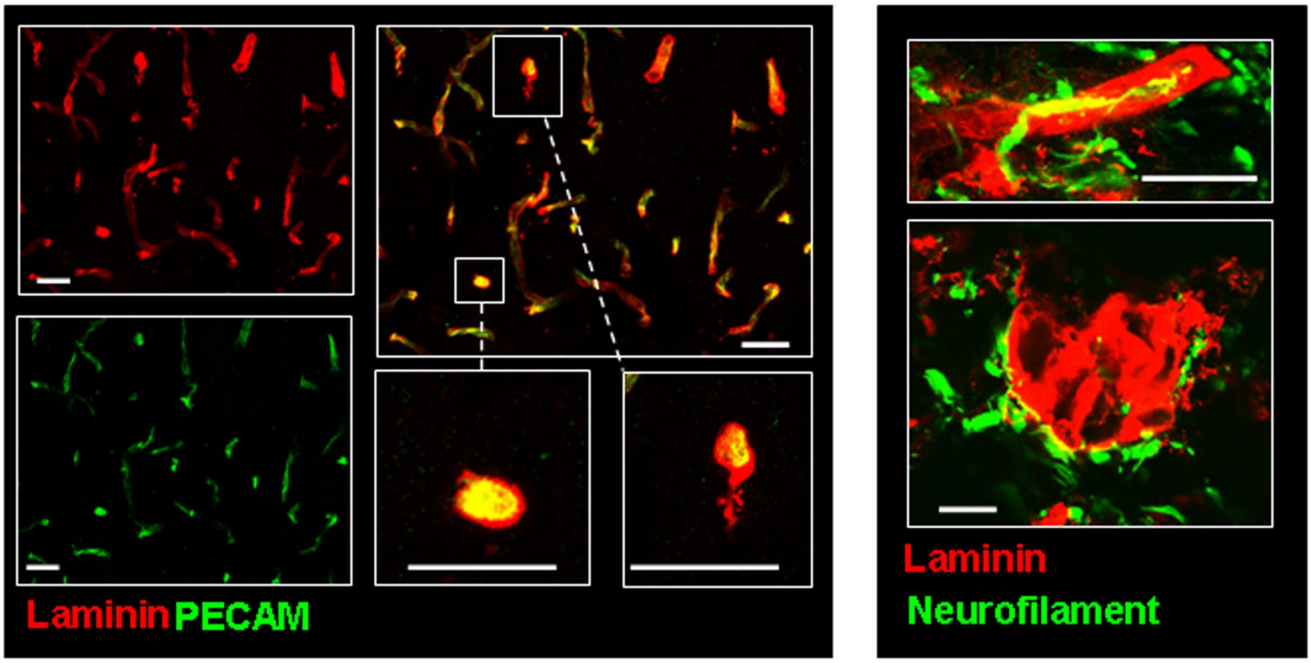

Vascular laminin as a substrate for axon growth

Fig. S5. Vascular laminin as a substrate for axon growth. *Left* panel: Horizontal spinal cord section immunostained for laminin (red) and PECAM (green) presented separated and overlaid on D7. Laminin was selectively found on and around (zoomed in images) blood vessels in the spinal cord. (Scale bar, 25 μm.) *Right* panel: Double immunostaining for laminin (red) and neurofilament (green) showing high densities of neurofilament in laminin-rich environment on D7. (Scale bar, 20 μm.) Altogether, these results suggest that vascular environment offers a good substrate to regrowing axons.

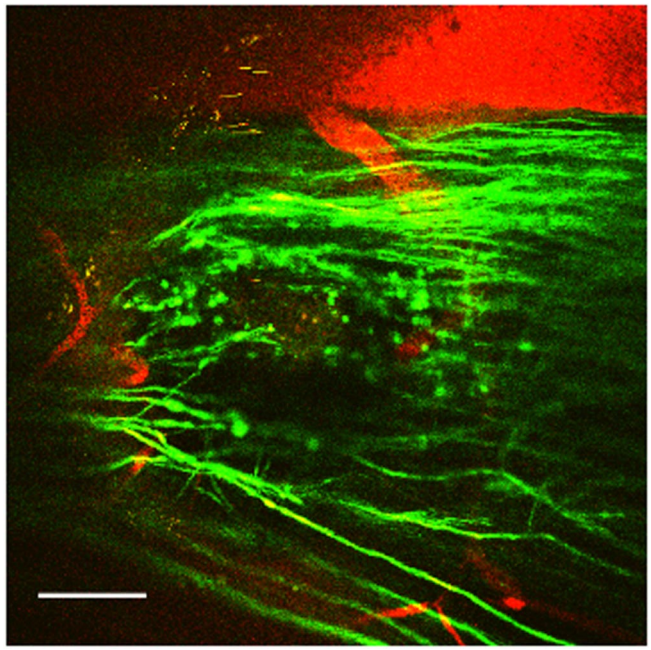

Movie S1. Acute degeneration of axons. Typical z-stack of images acquired in vivo every 5 μm over 150 μm depth immediately after lesion. (Scale bar, 100 μm.)

Movie S1 (GIF)

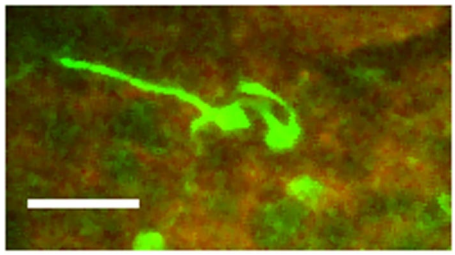

Movie S2. Time lapse of a FBV sprout development. Time lapse acquired on D6 every 20 min during 6 h. Note the development of a long sprout along the vessel whereas a short sprout directed toward the bottom of the image initially develops then quickly retracts. (Scale bar, 50 μm.)

Movie S2 (GIF)

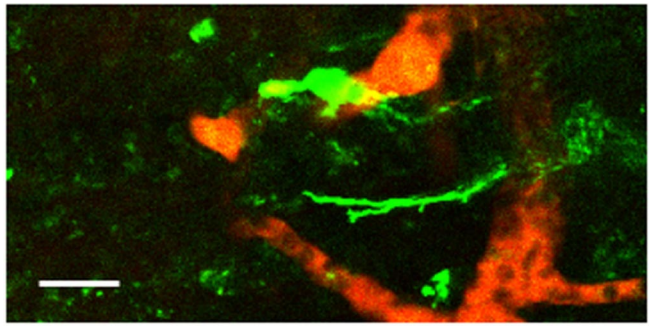

Movie S3. Time lapse of sprout development in a highly vascularized area. Highly dynamic sprouting and pruning of branches. Only the branch in contact with blood vessel is finally maintained. Note the development of 2 sprouts in opposite directions once the vessel surface is contacted. Time lapse acquired on D8 every 15 min for 6 h. (Scale bar, 50 μm.)

Movie S3 (GIF)

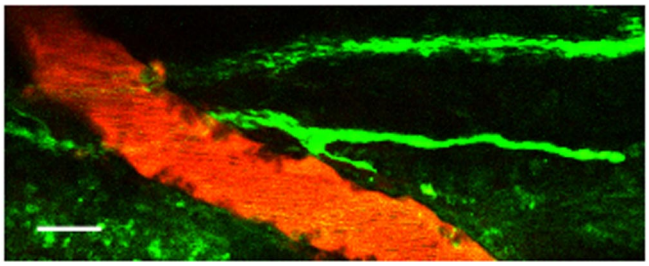

Movie S4. Time lapse of N-FBV and FBV sprouts. This N-FBV sprout did not grow over 3 h whereas a side branch developed along the blood vessel. Time lapse acquired on D8 every 15 min for 2.5 h. (Scale bar, 50 μm.)

Movie S4 (GIF)

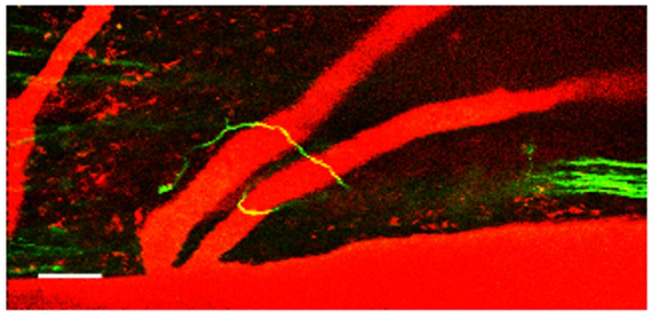

Movie S5. Inefficient trajectory of a FBV sprout. Z-stack of images acquired every 5 μm over a depth of 150 μm on D50. This FBV sprout wrapped itself around blood vessels resulting in an inefficient trajectory. (Scale bar, 50 μm.)

Movie S5 (GIF)

Table S1. VI as function of distance to lesion and time postlesion

	Distance to epicenter, μm				
Time postlesion, days	0–200	200–400	400–600	600–800	800–1,000
0	1.00	1.00	1.00	1.00	1.00
3	2.67	2.55	1.15	1.10	1.07
7	5.42	4.56	1.92	1.48	1.07
14	2.38	2.93	1.59	1.38	1.40
50	1.71	1.67	1.12	1.46	1.30
120	1.67	1.48	0.96	1.14	0.94

Table S2. Evolution of blood vessel distribution as a function of vessel diameter

	Distance to epicenter, μm														
	0–200			200–400			400–600			600–800			800–1,000		
Time postlesion, days	L	M	S	L	M	S	L	M	S	L	M	S	L	M	S
0	3.9	28.6	3.1	2.2	19.5	3.4	2.4	20.9	3.2	2.3	21.0	5.2	3.2	18.0	1.5
3	2.9	37.7	1.9	2.6	28.4	1.0	2.4	28.5	3.4	2.1	23.1	2.1	2.2	22.9	2.1
7	5.6	69.3	6.8	3.4	59.9	11.3	2.6	41.2	13.2	2.4	38.7	12.9	2.5	20.4	5.4
14	6.3	57.2	17.5	3.2	40.1	8.4	2.7	32.0	8.7	2.4	29.9	5.1	3.0	33.9	3.2
50	6.8	57.9	25.0	4.1	37.5	16.2	2.7	29.2	16.2	2.4	25.8	19.6	2.2	29.7	21.8
120	4.5	30.5	3.9	3.5	21	2.6	2.3	22.0	3.9	1.7	19.8	6.8	2.0	19.4	2

S, small; M, medium; L, large.